Chemical Physics Letters 513 (2011) 59–62

Contents lists available at ScienceDirect

Chemical Physics Letters

journal homepage: www.elsevier.com/locate/cplett

Effects of the dispersion interaction in liquid water

Omololu Akin-Ojo [a,*], Feng Wang [b]

[a] International Center for Theoretical Physics (ICTP), Strada Costiera 11, Trieste 34151, Italy
[b] Department of Chemistry, Boston University, Boston, MA 02215, USA

ARTICLE INFO

Article history:
Received 28 March 2011
In final form 19 July 2011
Available online 23 July 2011

ABSTRACT

The properties of liquid water obtained from molecular simulations using a density functional theory (B3LYP) based force field [O. Akin-Ojo, F. Wang, J. Comput. Chem. 32 (2011) 453.] with and without an intermolecular dispersion interaction term are compared. Although it is small, the dispersion interaction is found to significantly affect some properties such as the density and the heat of vaporization but not others, for example, the atom–atom radial distribution functions and the infrared spectra. The inclusion of the dispersion interaction in the force field produces an increase in the computed self diffusivity comparable to that resulting from a ~5 K rise in temperature.

1. Introduction

Since a water molecule has a large dipole moment, one might expect that the interaction between water molecules will be dominated by electrostatics and induction (polarization) with the dispersion interaction playing a minor role. Density functional theory (DFT) that is generally capable of modeling electrostatic interactions has been used extensively to simulate liquid water [1–18]. However, the exchange correlation functionals used in these simulations are local or semilocal and are incapable of describing the dispersion interaction. A survey of the literature indicates that these DFT based simulations typically underestimate the self-diffusivity of water and give atom–atom radial distribution functions (RDFs) that are more structured than the experimental ones. The work by Morrone and Car [19] has shown that the inclusion of quantum nuclear effects reduces the overstructuring of the RDFs. Since the exchange–correlation functionals used in the aforementioned simulations do not include long-range dispersion interactions, it is important to study the effects of the addition of a dispersion correction on the various simulated properties. Unless there is a cancellation of errors, the absence of dispersion interactions in typical exchange–correlation functionals might explain some of the differences between experimental results and those from *ab initio* molecular dynamics (MD) simulations.

Recently, some groups have performed *ab initio* MD simulations to examine the effect of the dispersion interaction in liquid water. Lin et al. (Ref. [20]) carried out *ab initio* MD simulations with the BLYP exchange–correlation functional and also augmented this with dispersion-corrected atom-centered potentials (DCACPs). DCACPs aim to rectify the lack of dispersion in a given functional but ultimately correct also for other defects in the functional [20,21]. These authors also performed simulations with the BLYP functional augmented with an empirical dispersion correction [22] according to Grimme. They reported a softening of the water structure upon inclusion of either DCACP or the empirical dispersion term and also an increase in the diffusion constant when the DCACP was used.

In another work, Schmidt et al. (Ref. [23]) performed *ab initio* MD simulations in the isothermal-isobaric ensemble and reported that both the PBE and BLYP functionals led to underestimates of the liquid density but the inclusion of an empirical dispersion correction [22] increased the calculated densities toward the correct experimental value.

Most recently, Wang et al. [24] investigated the effects of the dispersion interaction in liquid water by performing *ab initio* MD simulations with and without the inclusion of the nonlocal van der Waals correlation functional of Dion et al. [25]. They came to similar qualitative conclusions as Schmidt et al. [23] and Lin et al. [20] for the density and diffusion constant, respectively. Wang et al. argued that [24] the larger diffusion constant obtained in their study was because the van der Waals correlation functional increased the stability of non-hydrogen bonded dimers.

In this Letter, we study the effects of dispersion by simulating water with a potential created by force-matching the B3LYP potential energy surface (PES). With such a force field, a fairly large simulation box can be propagated on a B3LYP-quality PES for multi-nanoseconds to ensure convergence of all reported properties. This is a significant advantage over *ab initio* MD where one is limited to small simulation boxes and short simulation times due to the compute-intensive nature of *ab initio* methods. We report properties calculated at different temperatures, not only at room temperature.

The B3LYP potential energy surface used in this work has been reported in our previous publication [26]. In that work, a disper-

---

* Corresponding author.
E-mail addresses: oakin-oj@ictp.it (O. Akin-Ojo), fengwang@bu.edu (F. Wang).

0009-2614/$ - see front matter © 2011 Elsevier B.V. All rights reserved.
doi:10.1016/j.cplett.2011.07.064

sion correction term was added through an empirical correction term in a fashion similar to the so-called DFT-D approach [27,22]. The resulting force field was called B3LYPD-4F. In this Letter, we will perform simulations with the B3LYPD-4F potential but without the damped dispersion term. We will refer to this model as B3LYP-4F. The B3LYP-4F potential was fitted to the B3LYP potential energy surface directly through adaptive force matching but was never used in our previous work as a stand alone force field.

In this work, the effects of the dispersion interaction are examined by performing MD simulations with the "dispersionless" model (B3LYP-4F) and comparing the predicted properties of the liquid with those reported previously for the B3LYPD-4F potential along with experimental results from the literature.

2. Methodology

Details of the B3LYPD-4F force field were reported in Ref. [26]. In particular, the dispersion correction is of the form $-f(R)C_6/R^6$, where, R is the oxygen–oxygen distance. The coefficient $C_6 = 610.578$ kcal/mol was obtained from symmetry-adapted perturbation theory (SAPT) [28,29] at the level corresponding to the MP2 *ab initio* theory (second-order many-body perturbation theory with the Möller–Plesset partitioning of the Hamiltonian), i.e., the so-called $E^{(20)}_{\text{disp}}$ in SAPT. The parameters $c = 8.0$ and $R_m = 2.9$ Å of the damping function [27] $f(R) = 1/\{1 + exp[-c(R/R_m - 1)]\}$ were obtained from a fit to the differences between molecular forces/torques obtained from B3LYP and those from MP2 for water heptamers taken from snapshots of MD simulations [26].

Before going further, it is important to establish that, for molecules at large intermolecular separations, the dominant difference between the B3LYP and MP2 interaction energies is dispersion. Figure 1 shows the accuracy of our damped dispersion term in modeling the long-range part of the dispersion energy. In this figure, the differences between *ab initio* MP2 and B3LYP interaction energies for random dimers taken from configurations obtained in MD simulations are plotted against their O–O separations. Also included in this figure are the dispersion term $-C_6/R^6$, the damped dispersion term $-f(R)C_6/R^6$, and the SAPT $E^{(20)}_{\text{disp}}$ dispersion energy. As in Ref. [26], Dunning's aug-cc-pVTZ basis set [30] without the *d* functions on H and the *f* functions on O were used for the MP2, B3LYP, and $E^{(20)}_{\text{disp}}$ calculations. It is clear from this figure that at large intermolecular separations, the majority of the difference between B3LYP and MP2 is dispersion and our added semi-empirical term does a good job at reproducing this difference.

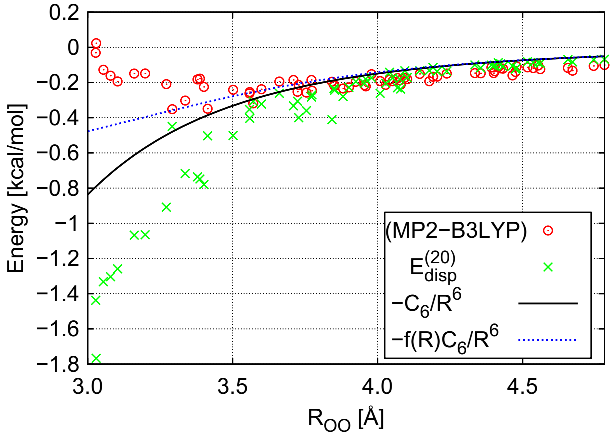

Figure 1. Differences between MP2 and B3LYP interaction energies for dimers taken from bulk simulations are plotted as a function of the O–O distance (R_{OO}). The corresponding $E^{(20)}_{\text{disp}}$, $-C_6/R^6_{\text{OO}}$, and damped dispersion $-f(R_{\text{OO}})C_6/R^6_{\text{OO}}$ are also shown.

In this Letter, the same procedure as used in Ref. [26] was followed to perform the simulations and calculate the properties. As a brief summary, the classical MD simulations were performed using the DL_POLY program [31]. A cubic box containing 216 water molecules was used, the electrostatic interactions were calculated with the Ewald method. The van der Waals cutoff radius was 9.0 Å. The radial distribution functions (RDFs) and heats of vaporization (ΔH_{vap}) were obtained from MD simulations in the canonical ensemble using a Nosé–Hoover thermostat with a time constant of 0.5 ps. Isothermal–Isobaric (i.e., constant-NPT) simulations were also performed to determine the density as a function of temperature using the Nosé–Hoover thermostat and barostat with time constants of 0.5 and 1.0 ps, respectively. To determine the infrared (IR) spectrum, centroid molecular dynamics simulations [32] were performed with an adiabaticity parameter of 0.05 and a timestep of 0.01 fs. Finally, for the diffusion constant (D_s), simulations were performed in the microcanonical ensemble.

3. Results

The IR spectra at ambient conditions calculated using the B3LYPD-4F and B3LYP-4F force fields are reported in Figure 2 along with the corresponding experimental spectra [33]. Little difference is observed in the calculated spectra from the simulations with and without dispersion. It is not surprising that the bending and stretching bands of B3LYPD-4F and B3LYP-4F are almost identical since these bands are determined mainly by intramolecular interactions which are the same for both force fields. The libration band is also identical within statistical uncertainty and this indicates that the libration is mostly determined by electrostatic and/or repulsion with the long-range dispersion playing an insignificant role.

Figure 3 reports the RDFs calculated using B3LYPD-4F and B3LYP-4F in MD simulations at 298.15 K. The experimental curves and the error bars from Ref. [34] are also plotted for comparison. It is clear from this figure that the RDF from both force fields are almost identical on the scale of the figure with the RDF without dispersion being arguably more structured. The differences between the RDFs from the B3LYPD-4F and B3LYP-4F models are negligible when compared with the experimental error bars. As Schmidt et al. remarked in Ref. [23], the small influence of dispersion on the RDFs is reminiscent of the work by Weeks et al. [35] who showed, for the Lennard–Jones fluid, that, at moderate to high densities, the attractive part of the force field has very little effect on liquid structure, i.e., the liquid structure is determined mainly by the repulsive

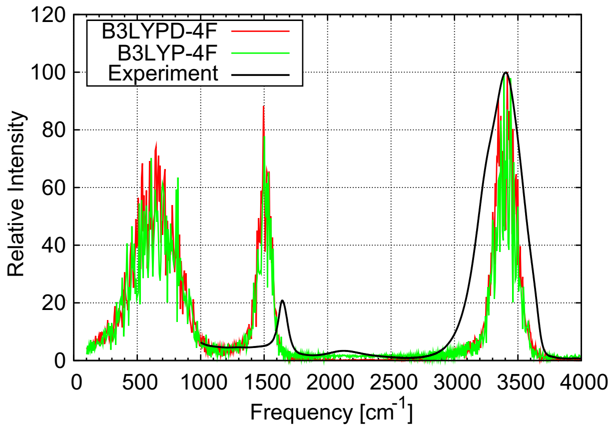

Figure 2. IR spectra calculated using the B3LYP-D and B3LYP based force fields. They were obtained from centroid MD simulations. The experimental results are from Ref. [33].